

Two-way coupling in a diffusive gas-particles turbulence: settling velocity and turbulence modification.

Laure Vignal ¹, Véronique Roig ¹, Livier Ben ¹, Jacques Borée ²

1. Institut de Mécanique des Fluides de Toulouse, UMR 5502 CNRS-INPT-UPS, Allée du Prof. Camille Soula, 31400 Toulouse, France

2. Laboratoire d'Etudes Aérodynamiques, ENSMA Poitiers, France

Abstract :

This paper describes experiments on the behavior of heavy particles in stationary diffusive air turbulence. The experimental apparatus consists in a vertical air jet confined in a tube closed at the top section, from where solid particles are injected uniformly. The study focuses on a region located at some distance from the nozzle, where, for the single-phase situation, turbulence is transported by turbulent diffusion. It is a region with a non homogeneous flow which has specific features: exponential decay of the various moments of the velocity, constant integral scale, isotropy and transverse homogeneity of the Reynolds stress tensor (Risso & Fabre, 1997). We used PIV/PTV 2D2C simultaneous measurements to analyze the interaction between the two phases in a range of Stokes numbers which generates clusters by preferential concentration. It results in a strong modification of the turbulence even if the volume fraction of the particles is low. We discuss the collective effects of the particles on turbulence as a cluster density effect.

1. Introduction

In the vast field of references devoted to the study of the interactions between phases in dilute dispersed particulate turbulent flows there are still a lot of unanswered questions. They concern the characterization of the regimes of preferential concentration (see Eaton & Fessler, 1994 for a review), the associated modification of the relative movement (Wang & Maxey, 1993) and the modification of the turbulence by two-way coupling (Ferrante & Elgobashi, 2003 ; Yang & Shy, 2005). Recent studies have shown that, in the presence of gravity, collective effects of the particles upon the fluid phase can consist in buoyancy-induced effects leading for example to a supplementary modification of the relative velocity as compared to the basic preferential segregation effect (Aliseda et al., 2002 ; Bosse & Kleiser, 2006). Such collective effects have not been pointed out previously, may be because it is difficult to study by experimental means the details of the interactions between the phases, and because numerical simulations of two-way coupling have mainly focused on the study of the mechanisms responsible for turbulence modification in the absence of gravity. Regimes where gravity effects are comparable to turbulence effects have not been explored precisely. We have thus performed an experimental study devoted to phase's interactions and collective effects in a gas-particulate turbulent flow where a competition between gravity and turbulence induced motions is present. A new experimental set-up has been defined and built. It had to achieve several aims. The first one was to obtain a turbulent gas-particulate flow where the turbulence is as simple as possible, in order to allow comparison with theoretical arguments or numerical simulations. The second constraint was to produce controlled

regimes of turbulence-particles interactions varying the Stokes number $St = \frac{\tau_p}{\tau_{turb}}$, and the ratio

characteristic of the relative importance of turbulence and gravity effects $\beta = \frac{U_{r\infty}}{u'}$ (where τ_p is the

relaxation time of the particles, τ_{turb} the integral time scale of turbulence, $U_{r\infty}$ is the terminal relative velocity and u' the rms velocity of the gas). The set-up and the measurements methods have also been defined to allow measurements of all the turbulent scales involved in the interactions

of both phases. We have thus built a new facility consisting in a vertical axi-symmetric jet confined in a tube closed at the top section, from where particles are injected uniformly (figure 1). And we have developed PIV (Particle Image Velocimetry) and simultaneous PTV (Particle Tracking Velocimetry) estimations in order to analyze the interactions between the phases. In § 2 we present the experimental set-up and the measurement methods. In § 3 we analyze the specificity of the single-phase diffusive turbulence which develops in the set-up. Then, we examine how the injection of particles in the flow modifies the turbulence even at low mass flow rate. As we conjecture that the modifications are related to the collective effects of the particles, an analysis of clusters presence is performed. Finally, we propose a model for generation of buoyancy-induced turbulence.

2. Experimental methodology

2.1. Flow facility

The experimental set-up has been described into details in Vignal et al. (2004-a). It consists in a vertical air jet confined in a tube closed at the top section, from where particles are injected uniformly (figure 1). The velocity of the jet at the inlet is U_0 , the diameter of the inlet section is $d=1\text{cm}$, the diameter of the tube is $D=9.8\text{cm}$, its high is $H=85\text{cm}$. The outlet section is located at the bottom of the tube. It is circular with an internal diameter $D'=9\text{cm}$ and an external diameter D . The 4 non dimensional parameters which characterize this flow are $\alpha=d/D$, $\beta=d^2/(D^2-D'^2)$, $\gamma=H/D$ and $Re=U_0d/\nu_f$. In the present study the velocity at the inlet of the jet was taken equal to $U_0=58\text{ m/s}$. Therefore these non dimensional numbers were very similar to the ones used by Risso & Fabre (1997) in their study for the single-phase case. In the single-phase case, at some distance from the nozzle a turbulent region develops where turbulence is transported by turbulent diffusion (located at $z/D>4.4$). It is a non homogeneous flow which has specific features: exponential decay of the various moments of the velocity, intense turbulence as compared to the mean motion, constant integral scale, isotropy and transverse homogeneity of the Reynolds stress tensor (Risso & Fabre, 1997). We have thus analyzed the interactions between particles and turbulence in this region. The particles injected from the top section are spherical glass particles with a mean diameter equal to $d_p=47\mu\text{m}$ (figure 2). Their density is $\rho_p=2460\text{kgm}^{-3}$. The injection system ensures a stationary and homogeneous injection of the particles. The mass flow rate of particles is $\dot{m}_p = 20\text{mg} / \text{s}$.

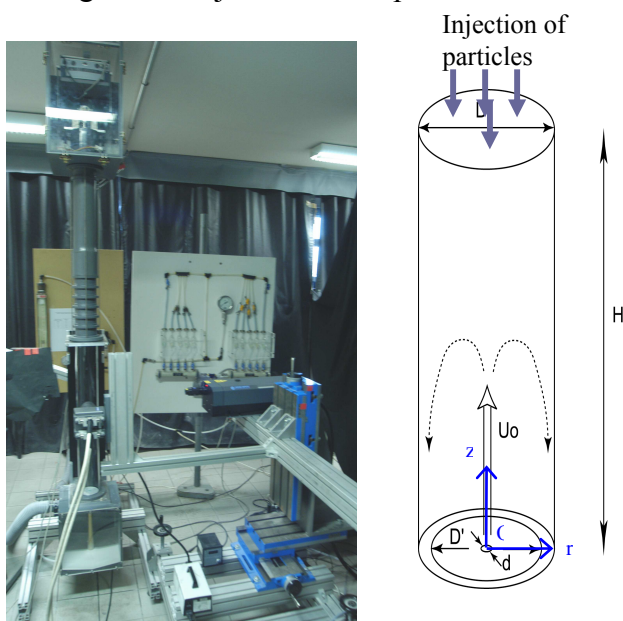


Figure 1 : View of the experimental set-up and scheme of the closed tube

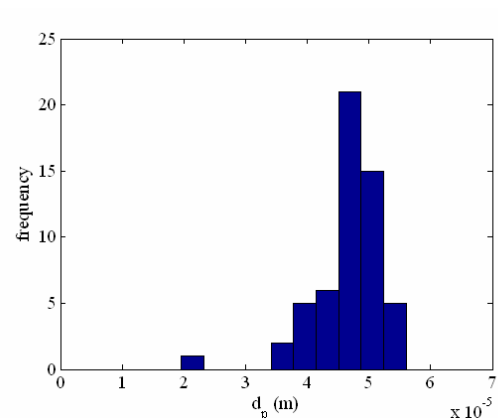


Figure 2 : Histogram of diameters of the glass particles (measurement with microscope)

2.2. PIV and PTV measurements in particulate turbulent flow

For PIV and PTV measurements, we used a 2×30mJ 2 ω Nd:Yag laser, a 1024×1280 pixels Sensicam PCO Sensicam camera with a CCD captor. The flow is seeded by oil tracers (1-2 μ m of diameter). We have developed a PIV /PTV 2D2C methodology similar to the one of Khalitov & Longmire (2002) in order to measure simultaneously the velocity fields of both phases. We acquire images with simultaneous presence of particles and tracers. The different stages of this PIV/PTV algorithm are discussed.

A- Separation of particles and tracers on the two-phase flow image by a thresholding technique, and generation of two different images adequate respectively for PIV and PTV image processing.

The choice of the threshold is based on the following analysis. We apply a very low threshold to the image, and we identify as an object any group of connected pixels above the threshold. We then collect the maxima of the grey levels of every object. The histogram of these maxima reveals a clear separation between the two populations of objects: the tracers and the particles (figure 3). The maximum grey levels of the tracers are low, those of the particles reach greater values. The threshold for the generation of images without particle for PIV treatments is chosen at the lowest limit of the separation between both populations (around 500 in figure 3).

B- PIV algorithm for the gas phase:

B-1 Generation of an image containing only the tracers:

The particles are replaced by substitutive image elements called “holes”. They are circular, black and their diameter is adapted to eliminate any halo effect on images.

B-2 Use of the standard PIV algorithm developed for single-phase flow (Maurel, 2001).

It consists in an iterative multigrid method with cell shifting and deformation. We have carefully chosen optimal parameters for PIV (ratio between mesh size and particle diameter, particle concentration...) to obtain accurate measurements in two-phase flow (Vignal *et al.*, 2004-a). We used 16x16 pixel (or 32x32 pixel) interrogation window size, and 50% of overlapping (or 75%).

B-3 Detection and elimination of false velocity vectors.

We have performed a supplementary test with images from DNS in two-phase flow (Fede *et al.*, 2004) to analyse the quality of the gas velocity vector measurements in the neighbourhood of the particles. We have compared the velocity from DNS to our PIV estimations near the particles for several densities of particles on the images, and we have defined the mean error as a function of the distance to the particle. The error is very important in the vicinity of the particles, but it diminishes with increasing distance to the particle (figure 4). It is minimum and constant for a distance greater than the mesh size of the first iteration (32 pixels). It is not equal to zero because the DNS calculation corresponds to a 8x8 pixels calculus. The application of the median filter eliminates a great amount of false vectors, and diminishes the error especially in the vicinity of the particles where the calculus was biased by the particle influence. However, the residual error is still too important (red symbols in figure 4), and we decided to eliminate any vector located in a 32x32 rectangular mask around any particle. We can thus expect a mean relative error less than 3% near the particles for a density of particles of 300 similar to the one in our experiments.

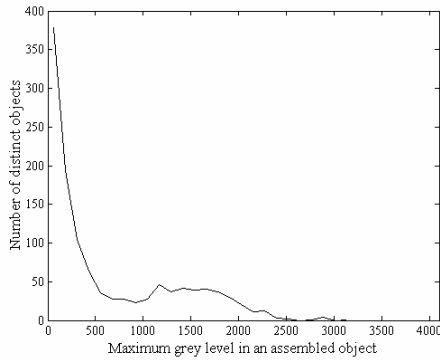


Figure 3 : Histogram of the maxima of the grey levels of the distinct objects in two-phase flow.

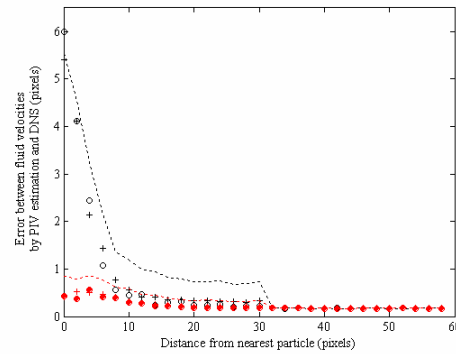


Figure 4 : Error in the fluid velocity estimation as a function of the distance to the nearest particle.

Test for several densities of particles : --- 900 particles/image; + 300 ; o 150.
 In black symbols : error *before* application of our median filter,
 In red symbols : error *after* application of our median filter.
 (mean displacement ≈ 7 pixels, 16×16 mesh size and 50% overlapping)

C- PTV algorithm for the particles:

We have developed a new algorithm for PTV that allows particle velocity measurements in dense groups of particles based on Keane *et al.* (1995) and Stellmacher *et al.* (2000). It has been tested and validated (Vignal *et al.*, 2004-a ; Vignal *et al.*, 2004-b). It uses images generated for PTV containing only the grey levels of the particles.

C-1 Pairing of the particles between two frames

For each particle number i located on the first frame the pairing consists in several stages. The first one is an estimation of the most probable velocity of the group of particles around it by PIV measurement in a large mesh centred on this particle (64×64 or 128×128 pixels). We use this velocity to locate a displaced window of research of the associated particle on the second frame denoted a_i . We search the best pairing in corresponding interrogation windows of size 20×20 pixels on each frame. Due to non negligible mass loading, several particles can belong to these windows. We thus examine any possible pairing in the group of particles. And we retain as the most probable the pairing which gives the less important variance of the velocities in the group. We then extract the couple of paired particles (i and a_i), and iterate the pairing operation for each particle. We also calculate the pairing from frame 2 to frame 1, and retain finally the pair of particles unchanged in this inversion.

C-2 Calculus of the velocity

Precise velocity is calculated by cross-correlation of very small regions around paired particle images (8×8 pixels); a cell shifting gives a precision of 0.1-0.2 pixel.

3. Results

We have validated our turbulent single-phase flow by a precise and satisfactory comparison with the reference results of Risso & Fabre (1997) (Vignal *et al.*, 2004). We report measurements in two-phase flows obtained with PIV/PTV windows centered on the axis and of extension $4 \text{ cm} \times 5 \text{ cm}$. The vertical upward axis is denoted z , the radial direction r , and the origin is at the exit of the air jet.

3.1. General description of the two-phase flow

3.1.1. Solid fraction distribution

We have estimated the volume fraction of the particles α_p from the measurement of the number of particles detected on the images. Because we did not have access to a measurement of the width of

the laser sheet (around 500 μm) we thus could only extract an approximate value of α_p . Figure 5 shows that it is nevertheless interesting, because we can see that in the region near the axis accessible to measurements the confined jet is composed of two parts: the region above $z/D=4$ is more concentrated, while the lower region is very dilute. In the upper part we have the order of magnitude $\alpha_p \approx 10^{-5}$. In such a range of volume fraction, it is expected from literature that the modification of the turbulence by two-way coupling is negligible (Wang & Maxey 1993, Fessler *et al.* 1994, Février 2000). We will see that it is not the case in this study where deep modifications are observed, like in the study of a dilute turbulent flow by Yang & Shy (2005).

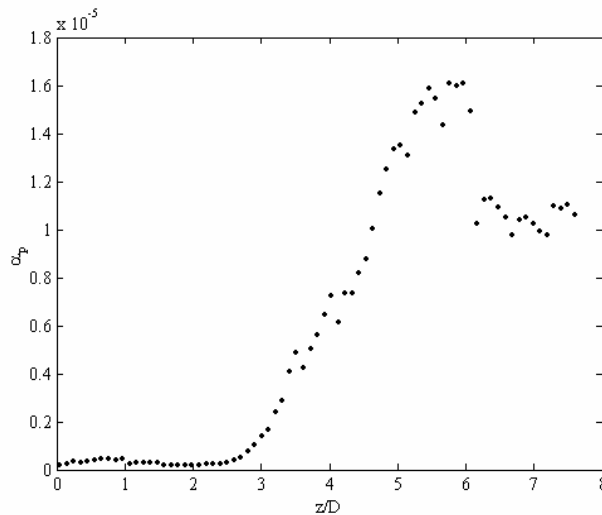


Figure 5 : Volume fraction of the solid phase in the vicinity of the axis

3.1.2. Non dimensional numbers for particles-turbulence interactions

The non dimensional parameters which characterize the interactions between the particles and the turbulence are plotted in figures 6 and 7 for $z/D > 2.5$ where we will focus our attention. The integral scales of the turbulence used to define St and Re_L have been evaluated by the measurement of the integral length scale L_{int} . As the particles cross the flow from top to bottom, they first cross a region where gravity dominates turbulence effects, and they then enter in a region where turbulence predominates more and more as indicated by the decrease of β . Their Stokes number increases when z decreases. For $z/D > 5$, even if the particles are quite responsive ($St < 0.1$), there is no doubt that they see a very low Reynolds number turbulence (figure 7).

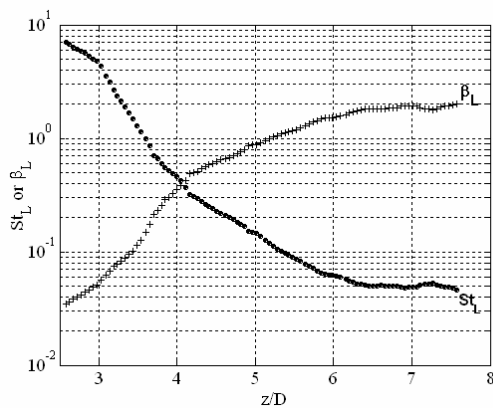


Figure 6: Longitudinal evolutions of St and β

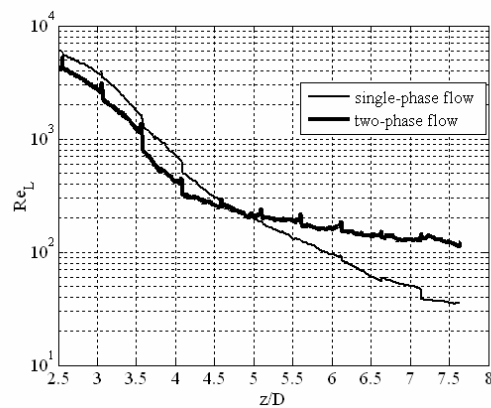


Figure 7: Longitudinal evolution of the Reynolds number of turbulence.

$$\left(Re_L = \frac{u' L}{\nu}, \text{ where } L \text{ is the integral length scale} \right)$$

3.1.3. Mean velocities in both phases:

The longitudinal evolution of the mean vertical velocity of the fluid $\overline{U_{zf}}$ near the axis is reported in figure 8 for the single-phase case and for the two-phase one. Due to the dilution of the lower part of the tube, there is no difference between the velocity of the gas in the single-phase and the two-phase flows for $z/D < 3.5$. From the exit of the jet, the axial velocity decreases due to transverse diffusion of the jet. Due to the walls of the tube, the rate of decrease is nevertheless lower than in an unconfined jet. Around $z/D = 3.6$, $\overline{U_{zf}}$ tends towards 0, and then reverses, before tending asymptotically towards 0 again. This is the signature of the presence of a recirculation zone in the upper part of the tube, with a downward flow near the axis (Figure 9).

For $z/D > 3.5$, the presence of particles modifies the velocity of the gas phase in the two-phase flow as compared to the single-phase flow and enhances the downward motion of the fluid. Transverse profiles of the mean velocities of the gas (not reported here) would indicate clearly that the mean flow is homogeneous in the transverse direction in the central region of the tube ($r/D < 0.2$).

The vertical mean velocity of the particles $\overline{U_{zf}}$ in the upper part of the flow ($z/D > 3$) results from the transport of the particles by the fluid and from a relative velocity which varies along the z axis. The precise analysis of the relative velocity is out of the scope of this contribution, but it is slightly different from the terminal particle velocity of -0.15m/s due to inertial effects. In the region of the jet ($z/D < 3$) the particles have an upward mean velocity like the fluid. But the longitudinal evolution of $\overline{U_{zf}}$ on the axis differs from the one of $\overline{U_{zf}}$ because the particles have to adapt themselves to the fluid accelerations. The noticeable difference of velocities near the inlet of the flow may be explained with the following argument similar to a discussion given by Prévost et al. (1996). The central part of the jet is very dilute and most of the particles fall at the periphery of the jet. Particles present in the jet, enter in it from a region of far lower velocity near $z/D = 0$, and they need time to reach the jet velocity level. Their relaxation motion thus explains that their averaged velocity is lower than the fluid velocity in this region.

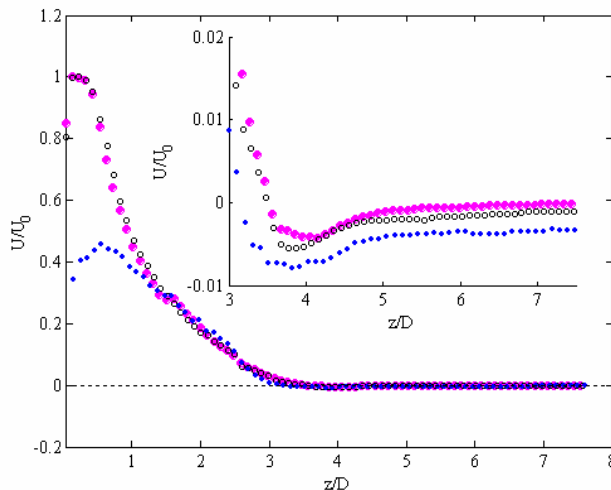


Figure 8: Longitudinal evolution of $U_z(r=0, z)$:
 ● : single-phase flow ; ○ : two-phase flow, gas ; ● : particles

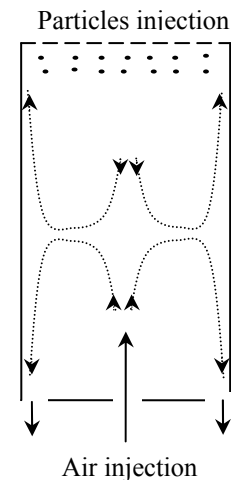


Figure 9 : Schematic diagram of the flow

3.1.4. Turbulence in both phases :

The second order moments of the velocity of the gas $\overline{u_{zf}^2}$ and $\overline{u_{rf}^2}$ measured along the axis in the single-phase flow have a typical evolution along the z axis that reveals the complex structure of the flow of a jet in a tube (figure 10). In the jet region, the strong shear stress generates high levels of

turbulence, which is anisotropic as in the free turbulent jet. Then the turbulence is attenuated, at a rate far lower than the mean flow, which will favour the study of the particles-turbulence interactions in the two-phase flow. At the same time, the redistribution between the components ensures a decrease of the anisotropy (figure 11). For $4.3 < z/D < 6.5$, the second order moments verify isotropic relation, and the turbulence is homogeneous in the transverse direction (not reported here). We also observed, as reported in figure 10, a specific property put into light and discussed in details by Risso & Fabre (1997), that in this region the moments decay following an exponential law. In the very high region of the tube ($z/D > 7$), the wall condition modifies these properties.

In the two-phase flow, the development of the dilute jet, generates exactly the same turbulence in the gas phase for $z/D < 4$ (figures 10 & 11) as compared to the single-phase flow. But the injection of particles from the top strongly enhances the level and the anisotropy of the turbulence in the top region ($z/D > 5$ or 5.5). Such a modification was unexpected for this dilute particle-gas flow, and we will discuss in the following the possible mechanisms for such a modification. In the region between $z/D = 4$ and 5.5, both turbulences joint themselves, which constitute also an interesting region where turbulence modulation by particles can be analysed with dominant turbulent effects. In this contribution we focus on the preliminary analysis of the generation of turbulence in the very high part of the flow.

In the two-phase jet ($z/D < 4$), the fluctuating motion of the particles is more anisotropic than the fluctuating motion of the fluid (figure 10). While the second order moment of their longitudinal velocity $\overline{u_{zp}^2}$ quite follows the evolution of $\overline{u_{zf}^2}$, their transverse moment $\overline{u_{rp}^2}$ is far more attenuated than $\overline{u_{rf}^2}$. This behaviour is characteristic of the dynamics of particles in a turbulent jet (Prévost *et al.*, 1996). In the high region of the tube ($z/D > 5.5$), $\overline{u_{zp}^2}$ is very similar to $\overline{u_{zf}^2}$, and $\overline{u_{rp}^2}$ to $\overline{u_{rf}^2}$ because the coupling between the phases is very strong in this region. The similarity of the turbulent components of each phase may come from the fact that the particles are responsive (their Stokes number is low (see figure 6)), and from a deep two-way coupling where the influence of the particles on the fluid phase is so strong that the fluctuating motions become strongly coupled.

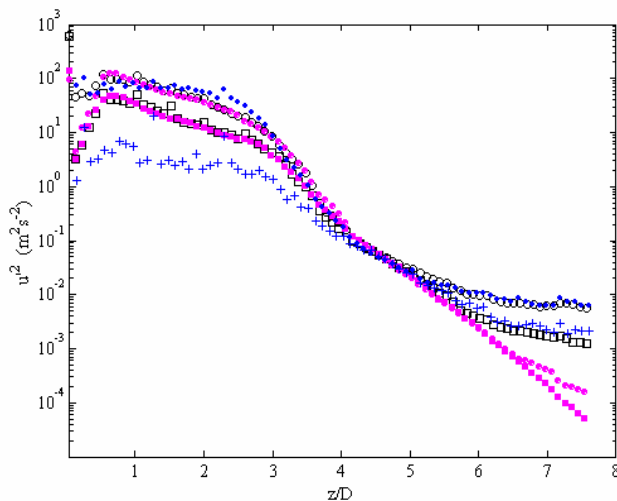


Figure 10 : 2d order moments of the velocity
 • : single-phase flow ; o : two-phase flow, gas ; • : particles
 $\overline{u_z^2}$ (o), $\overline{u_r^2}$ (• or +)

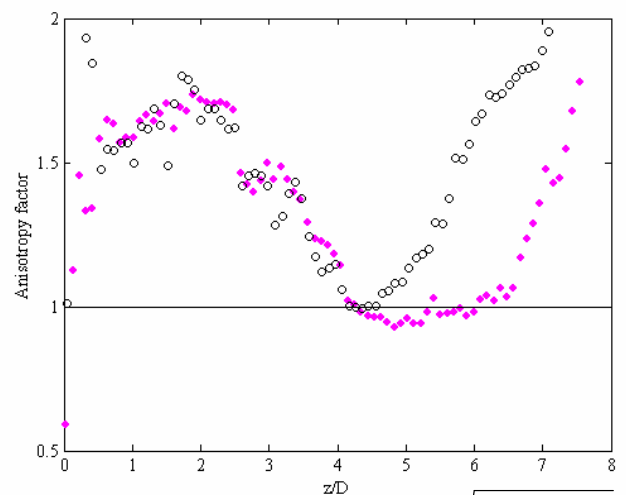


Figure 11 : Anisotropy factor $\sqrt{\overline{u_{zfaxe}^2} / \overline{u_{rfaxe}^2}}$
 • : single-phase flow ; o : two-phase flow

3.2. Mechanisms for the single-phase flow turbulence in the high region of the tube

For $4 < z/D < 6.5$ the equilibrium of turbulence in the single-phase case is very particular. Risso & Fabre (1997), have precisely analyzed this diffusive turbulence. They have shown that the transport equations of the Reynolds stresses reduce to equilibrium between turbulent diffusive transport terms and viscous dissipation terms. Two properties of turbulence are strongly correlated to this particular equilibrium : the constant values of the integral length scale, and the isotropy.

3.3. Modification of the two-phase flow turbulence in the high region of the tube

The deep modification of the turbulence in the region $z/D > 5$ leads to an inversion for the sign of the third order moment of the longitudinal velocity of the fluid $\overline{u'^3_{zf}}$ (for $z/D > 5.5$). It becomes negative, while in single-phase flow it remained positive, tending asymptotically towards 0. The modification of the probability density function of u'_{zf} at $z/D = 7.1$ denotes this asymmetry which is absent for the velocity component u'_{rf} or in the single-phase flow (figure 12). Such a modification points out that the diffusive transport of turbulence involved in the equilibrium of the single-phase turbulence is deeply modified in this region. Even if we have not analysed the transverse diffusive transport terms, it is clear that the diffusive equilibrium of the single-phase flow is completely destroyed because anisotropy is lost, and because the integral length scales are no longer constant.

The modification of the integral length scales due to the injection of particles is also noticeable (figure 13). In single-phase flow our measurements far from the top are in good agreement with the values of Risso & Fabre (1997) who explored the region $z/D < 6$. The presence of particles has a noticeable effect for $z/D > 5$ or 5.5, and while the longitudinal length scale is increased, the transverse one remains constant.

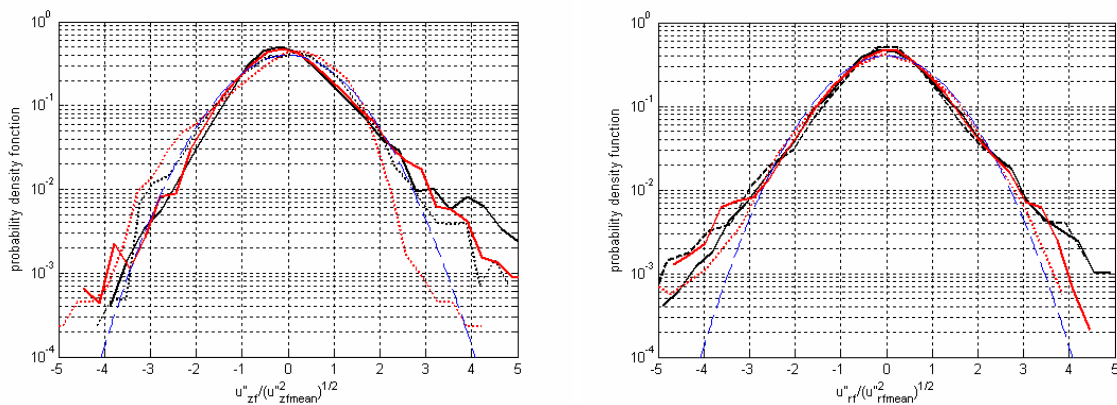
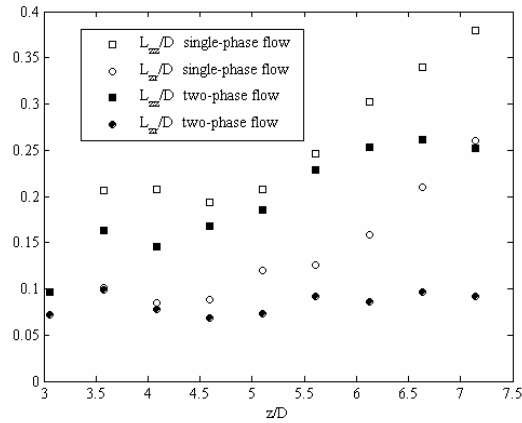


Figure 12 : Probability density functions of : a) $u'_{zf}/\sqrt{u'^2_{zf}}$ and b) $u'_{rf}/\sqrt{u'^2_{rf}}$
 — $z/D=4.6$, --- $z/D=7.1$, black : single-phase flow ; red : two-phase flow ; blue : Gaussian distribution

Figure 13: Integral length scales L_{int}

(L_{zz} is the longitudinal length scale, L_{zr} is the transversal one)

3.4. Preferential concentration

In the region $4 < z/D < 5$, β becomes more moderate and the value of St is near the critical value of 0.15 identified for preferential concentration to happen (Février, 2000) in developed turbulence. Indeed in this region the instantaneous visualizations of the particles positions show a deep heterogeneity (figure 14).

We have characterized the deviation of the particle concentration field from a statistically uniform random one, as in Fessler *et al.* (1994), by the estimation of a parameter denoted Dev . We divide the fields of observation into boxes of size ℓ . We count the number of particles in each box denoted N_i . We calculate the rms value of the number of particles per box (σ), and we compare this value to the rms value λ that a uniform random distribution would have ($\lambda = \sqrt{n}$ where n is the averaged number of particles per box). The parameter $Dev = \frac{\sigma - \lambda}{n}$ denotes the intensity of the deviation to

statistical homogeneity. It depends on the size of the box of analysis ℓ . When Dev is maximum the associated size ℓ denotes the more significant characteristic size of the clusters creating the deviation from uniformity. Figure 15 shows the evolution of Dev with the size ℓ at different z/D .

Noticeable values of Dev are measured for $3.6 < z/D < 7.4$. This denotes that a heterogeneous field of concentration exists in this region. The very important values of Dev for $z/D < 4.8$ show that preferential concentration is statistically dominant in this region. It is maximum near $z/D=4$ where $St \approx 0.3$ (and $\beta \approx 0.3$), while usual criteria provide a maximum preferential concentration for $St \approx 0.15$ (Février, 2000). This critical value is obtained at $z/D \approx 5$. The deviation may be explained because $\beta \approx 0.9$ at $z/D=5$, meaning that particles cross the vortices in a time equivalent to their turn-over time, so that preferential segregation cannot be very efficient. For $z/D > 4.75$, values of Dev are less important, but we detect a deviation to statistical homogeneity. Up to $z/D=5.75$ a typical length scale associated to a maximum still remains and is unchanged. But above this section it is more difficult to detect a preferential size of heterogeneity, while important values of Dev still reveals the presence of heterogeneity. The detected size of the clusters is constant in the region $4 < z/D < 5.9$, it is about $\ell = 8$ or 10 mm. This value is equal to $25-34\eta_{kolm}$ (for $4.3 < z/D < 5.4$, where η_{kolm} is the Kolmogorov length scale) in agreement with Fessler *et al.* (1994) or Yang & Shy (2005).

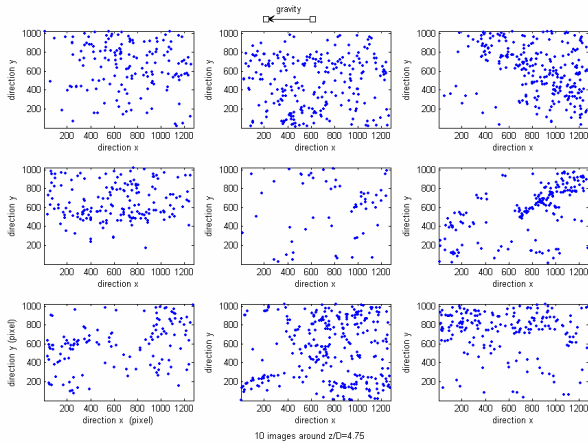


Figure 14: Visualizations of the particles positions at various instants in a window located around $4.5 < z/D < 5$.

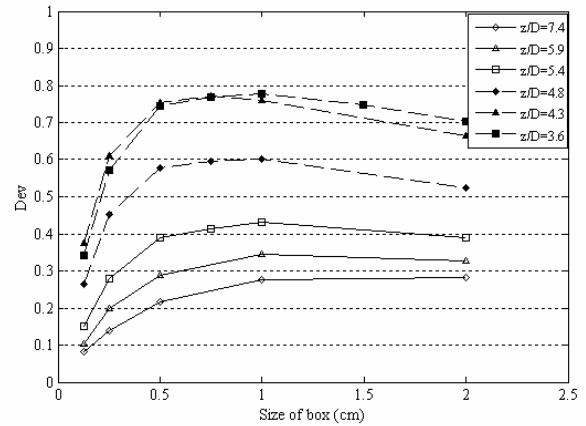


Figure 15: Parameter Dev characterizing the deviation from homogeneity.

Some visualisations (figure 16) confirm that the particles, when they are preferentially concentrated, are essentially found at the periphery of the vortices as shown by several authors (Squires & Eaton, 1990 for example). Qualitative estimations also confirm that on the average, clusters contain over-concentrations of about $5-9 \alpha_p$, an order of magnitude in agreement with the values of 2.5-3 given by Aliseda *et al.* (2002).

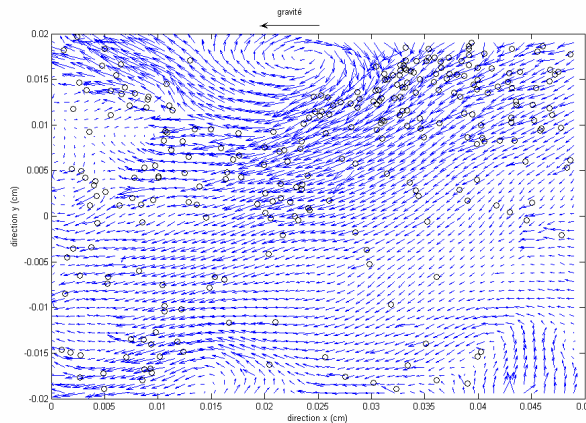


Figure 16: Localisation of the particles in the velocity field of the fluid (around $z/D=4.75$).

3.5. A model for buoyancy induced two-way coupling

The strong modification of the turbulence intensity and anisotropy for $z/D > 5$ or 5.5 cannot be explained by usual two-way coupling terms representing the power developed by the drag force on an isolated particle, in the fluctuating and averaged relative movements. Indeed, both terms compensate (Vignal, 2006). Another mechanism for production of turbulence by collective effects is proposed here. We consider that we can model the interactions of the large-scale fluctuations of the particle concentration with the surrounding fluid by modelling the associated more or less well-defined clusters like denser fluid regions. Such a model has been successfully proposed by Aliseda *et al.* (2002) to explain the enhancement of the mean relative velocity with concentration variations when preferential concentration develops. The basic mechanisms for modification of turbulence are therefore very similar to the generation mechanisms for homogeneous buoyancy-induced turbulence analysed for example by Batchelor *et al.* (1992) where density fluctuations, without a mean density gradient, generate a well-defined turbulence.

We thus define a mixing density $\rho = c\rho_p + (1-c)\rho_f$ where c is the local and instantaneous volume fraction of particles. We consider that in the high part of the tube the flow may be assumed as quasi-homogeneous. Thus, the turbulent kinetic energy equation reduces to the equilibrium relation:

$$\overline{g u_z' \rho'} = \overline{\rho \varepsilon}$$

with $\overline{\rho} = \alpha_p \rho_p + (1 - \alpha_p) \rho_f \approx \rho_f$ for the mixing, and α_p the averaged volume fraction ($\approx 1.5 \cdot 10^{-5}$), $\rho' = (c - \alpha_p) \rho_p - (c - \alpha_p) \rho_f \approx (c - \alpha_p) \rho_p = c' \rho_p$ the fluctuation of density of the mixing which simplifies due to the contrast of densities, ε the viscous dissipation rate, and u_z' the vertical velocity fluctuation in the gas. We take: $\varepsilon = \frac{\alpha k^{3/2}}{L_{\text{int}}}$, where k is the turbulent kinetic energy, and L_{int} the integral length scale. α is a positive constant value near unity.

We introduce a correlation coefficient $c_{u\rho}$ between u_z' and ρ' : $\overline{u_z' \rho'} = c_{u\rho} \overline{u_z'^2}^{1/2} \overline{\rho'^2}^{1/2}$. The value of $c_{u\rho}$ is assumed near unity. We also introduce the anisotropy factor $\gamma = \frac{\overline{u_z'^2}}{\overline{u_r'^2}} \approx \frac{\overline{u_z'^2}}{\overline{u_\theta'^2}}$. The kinetic energy k thus writes: $k = \frac{\gamma + 2}{2\gamma} \overline{u_z'^2}$. And the turbulent kinetic energy equilibrium relation thus leads:

$$k = \frac{c_{u\rho}}{\alpha} \sqrt{\frac{\gamma + 2}{2\gamma}} g L_{\text{int}} \frac{\overline{\rho'^2}^{1/2}}{\rho_f}$$

We have measured γ values around 4 comparable to the values of Batchelor *et al.* (1992) (≈ 2.8). Using the measured integral scale ($L_{\text{int}} = 2.5 \text{ cm}$) and the over-concentration of particles present in the clusters, we can compare the measured values of k to this model. We consider that the main contribution to density variations is due to clusters contributions and we write: $\overline{\rho'^2}^{1/2} \approx (c_{\text{cluster}} - \alpha_p) \rho_p$. We also take $c' \approx (c_{\text{cluster}} - \alpha_p) \approx 1.5$ to $2 \alpha_p$ (Aliseda *et al.*, 2002) because our qualitative estimations are too imprecise but in agreement with the results of Aliseda *et al.* We thus obtain the following value: $k \approx 0.97 \cdot 10^{-2}$ to $1.3 \cdot 10^{-2} \text{ (m/s)}^2$. This estimation is in very good agreement with the measured values of k ($z/D > 5$) (figure 10).

This mechanism of generation of turbulence is thus pertinent in our flow. It is due to particle concentration fluctuations when preferential concentration is present in the field of gravity acceleration. It is a two-way coupling mechanism which is dominant, even at very low particle volume fraction, in the present situation where $\beta \geq 0.8$ or 1 and where the other production mechanisms are vanishing.

4. Conclusion

We have discussed new experimental results on particle-laden turbulence, obtained with optical methods in diffusive turbulence. Careful development of simultaneous measurements of the velocities of both phases by a PIV/PTV 2D2C methodology was achieved. At low mass flow rate, in our experimental conditions where $\beta = \frac{U_{rms}}{u'}$ is not negligible, we observed a great modification of the turbulence when adding particles to the gas flow. The turbulent kinetic energy is enhanced, and a strong anisotropy appears in the flow. Several arguments indicate that the modifications can be related to the collective effects of the particles. An analysis of clusters presence is performed, which confirms the presence of preferential concentration. We propose a model for generation of buoyancy-induced turbulence associated to these clusters effects. This model is in good agreement with the experimental results.

References

- Aliseda A., Cartellier A., Hainaux F., Lasheras J.C., (2002), Effect of preferential concentration on the settling velocity of heavy particles in homogeneous isotropic turbulence, *J. Fluid Mech.*, vol. 468, pp. 77-105.
- Batchelor G. K., Canuto V. M., Chasnov J. R., (1992), Homogeneous buoyancy-generated turbulence, *J. Fluid Mech.*, vol. 235, pp. 349-378.
- Bosse T., Kleiser L., (2006), Small particles in homogeneous turbulence: Settling velocity enhancement by two-way coupling, *Phys. Fluids* 18.
- Eaton J. K., Fessler J. R., (1994), "Preferential concentration of particles by turbulence." *Int. J. Multiphase Flow* 20 (Suppl.): 169 - 209.
- Fede P., Février P. and Simonin O. (2004). Numerical study of the effect of the fluid turbulence microscales on particle segregation and collision in gas-solid turbulent flows". 5th ICMF, Yokohama, Japan
- Ferrante A., Elgobashi S., (2003), On the physical mechanisms of two-way coupling in particle-laden isotropic turbulence, *Phys. Fluids* 15 (2): 315 – 329.
- Fessler J. R., Kulick J. D., Eaton, J. K., (1994), "Preferential concentration of heavy particles in a turbulent channel flow." *Phys. Fluids* 6(11): 3742 - 3749.
- Février P., (2000), Etude numérique des effets de concentration préférentielle et de corrélation spatiale entre vitesses de particules solides en turbulence homogène isotrope stationnaire, INPT PhD, Toulouse, France
- Keane R.D., Adrian R.J. and Zhang Y. (1995), Super-resolution particle imaging velocimetry, *Meas. Sci. Technol.* 6: 754 – 768.
- Khalitov D. A., Longmire E. K., (2002), Simultaneous two-phase PIV by two-parameter phase discrimination, *Volume 32, Number 2*, pp. 252 – 268.
- Maurel S. (2001). "Etude par imagerie laser de la génération et de la rupture d'un écoulement tourbillonnaire compressé. Situation modèle pour la validation de simulations aux grandes échelles dans les moteurs". Thèse INPT / IMFT. Toulouse, France.
- Prévost F., Boree J., Nuglisch H. J., Charnay G., 1996, "Measurements of fluid/particle correlated motion in the far field of an axisymmetric jet", *Int. J. Multiphase Flow*, vol 22, n°4, pp. 685-701.
- Risso F. and Fabre J. (1997), "Diffusive turbulence in a confined jet experiment." *J. Fluid Mech.* 337: 233 - 261.
- Squires K., Eaton J. K., 1990, Particle response and turbulence modification in isotropic turbulence, *Phys. Fluids*, 2, pp. 1191-1203.
- Stellmacher M. and Obermayer K., (2000), A new tracking algorithm based on deterministic annealing and alternative distance measures. *Experiments in Fluids* 28: 506 – 518
- Vignal L., Ben L., Roig V., Bazile R., Borée J., (2004-a), Experimental study of a particulate turbulent confined jet by optical methods, 12th Int. Symposium on Applications of laser techniques to fluid mechanics, Lisbon, Portugal.
- Vignal L., Ben L., Cazin S., (2004-b), "Validation de mesures couplées PIV-PTV en écoulement turbulent diphasique gaz-particules", 9^{ème} Congrès Francophone de Vélocimétrie Laser, Bruxelles, Belgique.
- Wang L.P., Maxey M. R., (1993), Settling velocity and concentration distribution of heavy particles in homogeneous isotropic turbulence, *J. Fluid Mech.*, vol. 256, pp. 27-68.
- Yang T.S., Shy S.S., (2005), Two-way interaction between solid particles and homogeneous air turbulence : particle settling rate and turbulence modification measurements, *J. Fluid Mech.*, vol. 526, pp. 171-216.
- Vignal L., (2006), Chute d'un nuage de particules dans une turbulence diffusive : Etude des couplages entre phases par diagnostics optiques, INPT PhD, Toulouse, France, to be defended on July, the 7th.